Applied Mathematics & Information Sciences
An International Journal

http://dx.doi.org/10.18576/amis/200205

A Novel Brain Tumor Segmentation Approach Based on Combining Fine-Tuned Deep Learning and Augmentation Techniques

Hanan H. Amin[1,*], *E. A. Zanaty*[1], *and Walaa M. Abd-Elhafiez*[2,3]

[1]Information Technology Department, Faculty of Computers and Artificial Intelligence, Sohag University, Sohag, Egypt
[2]College of Engineer and Computer Science, Jazan University, Jazan, Kingdom of Saudi Arabia
[3]Computer Science Department, Faculty of Computers and Artificial Intelligence, Sohag University, Sohag, Egypt

Received: 7 Nov. 2025, Revised: 25 Dec. 2025, Accepted: 31 Jan. 2026
Published online: 1 Mar. 2026

Abstract: Recently, brain tumor diagnosis has increasingly relied on medical image analysis, providing essential inputs for diagnosis, prognosis, and treatment planning. Deep learning models are an important method used to predict patient progression, impacting the selection of effective medical prescriptions. Deep learning models have achieved impressive results in automatic classification, but diverse datasets face challenges in achieving high generality and robustness. In this paper, we propose a new approach that combines fine-tuning of hyperparameters with advanced computational scripting techniques to increase segmentation accuracy. In this case, we adopted a modified FCNN architecture to systematically adjust learning speeds, batch size, dropout, and optimizer parameters. We incorporated data scripting strategies such as rotation, flipping, density variation, and elastic deformation to increase dataset diversity. This combination helps improve the performance of deep learning models when applied to a wide variety of datasets and study samples. The proposed method was evaluated on the Brats 2020 dataset and compared to existing methods, including Patchnet, Deeplabav3, and Baseline FCNN. The results indicate that our augmented model improves state-of-the-art methods in terms of Dice coefficients, accuracy, and memory. The results demonstrate the effectiveness of combining computer-centric and model-centric adaptation strategies for improving brain tumor segmentation.

Keywords: Brain Tumor; Segmentation; Fine-Tuned Parameters; Deep Learning; PatchNet; DeepLab; FCNN.

1 Introduction

Brain tumors are among the most severe and life-threatening medical conditions, necessitating accurate and efficient diagnosis and treatment strategies. These tumors can be primary, originating in the brain, or metastatic, spreading from other parts of the body. Regardless of their origin, brain tumors pose significant challenges due to their complex structure, variability in size and location, and the critical nature of the brain as an organ [1]. Accurate segmentation of brain tumors in clinical imaging is vital for surgical planning, radiotherapy, and monitoring disease development. Segmentation involves delineating tumor regions from surrounding healthy tissue, which is crucial for determining the quantity of the tumor, making plans for surgical interventions, and assessing treatment efficacy [26].

Traditional segmentation methods rely on manual annotations by radiologists, which can be subjective, time-consuming, and prone to inter-observer variability. Manual segmentation requires significant expertise and is often inconsistent due to differences in interpretation among radiologists [18]. Moreover, the increasing volume of medical imaging data in clinical practice has made manual segmentation impractical, highlighting the need for automated and reliable segmentation methods.

With the rise of artificial intelligence (AI), deep learning-based segmentation methods have shown remarkable success in improving the accuracy and efficiency of brain tumor segmentation. Deep learning models, especially convolutional neural networks (CNNs), have become the cornerstone of automated

* Corresponding author e-mail: hanan.hamed@fci.sohag.edu.eg

medical image analysis. These models can research complicated styles and functions from huge datasets, enabling them to perform responsibilities that include classification, detection, and segmentation with high precision [3]. Architectures such as Fully Convolutional Networks (FCNN) [10], U-Net [4], and DeepLab [25] have demonstrated substantial improvements in segmenting brain tumors from MRI scans [5], [6]. For instance, the U-Net architecture, introduced by Ronneberger et al. [4], has become a benchmark for medical image segmentation due to its encoder-decoder structure and skip connections, which preserve spatial information and improve segmentation accuracy.

Despite these improvements, demanding situations stay in making use of deep learning models for brain tumor segmentation. One major challenge is the limited availability of labeled datasets. Annotating medical images is a labor-intensive process that requires expertise, and the resulting datasets are often small compared to those used in other domains of AI [6]. This limitation can lead to model overfitting, wherein the model performs well on the training data but fails to generalize new, unseen data. Additionally, variability in MRI scans due to differences in acquisition protocols, scanner types, and imaging parameters can similarly complicate the segmentation task [5].

To address these challenges, researchers have explored various strategies, consisting of switch getting to know, information augmentation, and hyperparameter optimization. Transfer learning involves fine-tuning pre-trained models on new datasets, allowing the model to leverage knowledge from larger datasets. Data augmentation enhances model robustness by artificially increasing the size and diversity of the training dataset through transformations such as rotation, flipping, elastic deformations, and contrast adjustments [8]. These techniques help the model generalize better to new data and reduce overfitting. Hyperparameter optimization, on the other hand, involves tuning parameters such as learning rates, dropout rates, batch sizes, and activation functions to improve model convergence and performance [9].

In this study, we investigate how fine-tuning hyperparameters and augmenting training datasets can enhance the performance of deep learning models in brain tumor segmentation. We compare our approach with existing models such as PatchNet, DeepLab, and FCNN to evaluate improvements in segmentation accuracy and generalizability. By leveraging a combination of optimized deep learning models and data augmentation techniques, we aim to provide a more effective and reliable method for brain tumor segmentation, ultimately assisting clinicians in more precise diagnosis and treatment planning. The rest of this paper is organized as follows. Section 2 discusses previous studies, Section 3 explains the data and methods we used, Section 4 covers the models we tested, and Section 5 outlines how we improved them. Section 6 describes the training process, Section 7 introduces our approach, Section 8 explains how we measured performance, Section 9 presents the results, and the Conclusion summarizes our findings and future work.

2 Related Work

Medical imaging analysis uses new safety technologies like computed tomography (CT), magnetic resonance imaging (MRI), and positron emission tomography (PET) to diagnose patients and preserve lives. The four MRI image modalities are T1-weighted, T2-weighted, T1-weighted with contrast enhancement (T1ce), and fluid-attenuated inversion recovery (FLAIR). Each modality is represented as a 2D slice, and when all the slices are combined, a 3D representation of the brain is generated. Segmenting the brain tumor using a variety of modalities and sequencing can enhance outcomes and yield complementary features on areas of various sub-gliomas. In the field of brain tumor segmentation, semi-automatic and automatic methods have been presented; the automatic method demonstrated its effectiveness and a great potential for more reliable and accurate outcomes.

The field of medical image segmentation has seen significant advancements with the introduction of deep learning architectures. These models have demonstrated remarkable success in automating the segmentation of complex structures, including brain tumors, by learning hierarchical features [28] from large datasets. Below, we discuss several key deep learning architectures and their contributions to medical image segmentation, with a focus on brain tumor segmentation.

Convolutional networks (CNNs) were among the first deep learning architectures designed for pixel-wise segmentation tasks. Long et al. [10] introduced CNNs by replacing fully connected layers in traditional CNNs with convolutional layers, enabling the network to produce spatial output maps instead of classification scores. This architecture laid the foundation for many subsequent segmentation models. CNNs have been widely adopted in medical imaging due to their ability to handle variable input sizes and produce dense predictions. However, their performance is often limited by the loss of fine-grained spatial details due to repeated pooling operations.

The U-Net architecture, introduced by Ronneberger et al. [4], revolutionized medical image segmentation by addressing the limitations of FCNNs. U-Net features an encoder-decoder structure with skip connections that bridge the gap between the contracting path (encoder) and the expansive path (decoder). The encoder extracts high-level features through convolutional and pooling layers, while the decoder reconstructs the segmentation mask using upsampling and convolutional layers. The skip connections preserve spatial information, enabling the model to produce precise segmentation masks even with limited training data. U-Net has become the gold

standard for medical image segmentation and has been extensively applied to brain tumor segmentation tasks [5].

While 2D CNNs process individual slices of volumetric data, 3D CNNs extend this approach to handle entire 3D volumes, capturing spatial context across multiple slices. Kamnitsas et al. [6] proposed a multi-scale 3D CNN architecture for brain tumor segmentation, which leverages 3D convolutions to model volumetric dependencies. Their model achieved state-of-the-art results on the BraTS dataset by combining multi-scale features and fully connected conditional random fields (CRFs) for post-processing. However, 3D CNNs are computationally intensive and require significant memory resources, limiting their applicability in resource-constrained settings.

DeepLab, introduced by Chen et al. [25], is another influential architecture for semantic segmentation. It employs atrous (dilated) convolutions to capture multi-scale contextual information without increasing the number of parameters. DeepLab also incorporates a fully connected CRF to refine segmentation boundaries. While originally designed for natural image segmentation, DeepLab has been adapted for medical imaging tasks, including brain tumor segmentation. Its ability to handle large receptive fields makes it suitable for capturing the diverse appearance and size of brain tumors.

Patch-based methods, such as PatchNet, divide the input image into smaller patches and process them independently. This approach reduces memory requirements and allows the model to focus on local features. Zhao et al. [27] proposed a patch-based CNN for brain tumor segmentation, which achieved competitive results on the BraTS dataset. However, patch-based methods often struggle to capture global context, which is crucial for accurate segmentation of large or irregularly shaped tumors.

Attention mechanisms have been integrated into deep learning models to improve segmentation performance by focusing on relevant regions of the input image. Oktay et al. [13] introduced attention gates in U-Net, which dynamically highlight important features while suppressing irrelevant ones. This approach has been shown to enhance segmentation accuracy, particularly for small or poorly contrasted tumor regions.

Generative Adversarial Networks (GANs) have been explored for medical image segmentation, particularly in scenarios with limited labeled data. GANs consist of a generator and a discriminator, which are trained simultaneously in a competitive manner. The generator produces segmentation masks, while the discriminator evaluates their quality. Xue et al. [14] proposed a GAN-based model for brain tumor segmentation, which demonstrated improved performance by leveraging adversarial training to produce more realistic segmentation masks.

Transfer learning has emerged as a powerful strategy for medical image segmentation, particularly when labeled data is scarce. By fine-tuning pre-trained models on new datasets, transfer learning enables the model to leverage knowledge learned from larger, more diverse datasets. Havaei et al. [7] demonstrated the effectiveness of transfer learning for brain tumor segmentation, achieving state-of-the-art results by fine-tuning a pre-trained CNN on the BraTS dataset [26].

Data augmentation techniques have been widely adopted to address the limited availability of annotated medical images. Perez and Wang [8] highlighted the effectiveness of data augmentation in improving model generalization and robustness. Common augmentation techniques for brain tumor segmentation include rotation, flipping, scaling, elastic deformations, and intensity transformations. These techniques artificially increase the size and diversity of the training dataset, reducing the risk of overfitting and improving segmentation accuracy.

Wang et al. introduced TensorMixup, a novel statistics augmentation method that blends three-D MRI patches with the usage of tensors sampled from a Beta distribution. Applied to a 3-D U-Net structure, this method executed Dice scores of 92.15%, 86.71%, and 83.49% for entire tumor, tumor core, and enhancing tumor regions, respectively, demonstrating its efficacy in glioma segmentation [39].

In the context of the BraTS 2023 undertaking [38], Ferreira et al. employed generative adversarial networks (GANs) and registration-based techniques to synthetically augment training records. Their ensemble technique, combining nnU-Net, Swin UNETR, and former BraTS-triumphing models, carried out Dice ratings of 0.9005, 0.8673, and 0.8509 for complete tumor, tumor core, and enhancing tumor, respectively, highlighting the potential of synthetic data in enhancing segmentation overall performance [38].

Fine-tuning pre-trained fashions has additionally been pivotal. Asiri et al. [37] utilized an exceptionally tuned Vision Transformer (ViT) for mind tumor detection in MRI scans, achieving excessive accuracy and performance, underscoring the advantages of adapting transformer-primarily based architectures to clinical imaging responsibilities.

In addition, Zeinelldin and Mathis-Hulrich proposed HT-CNNS architecture, with hybrid transformers and conversion of neural networks adapted through transmission learning. His approach demonstrated better classification results in different brain tumor types, which emphasize the versatility of the fine-tuning hybrid model [24].

The evolution of deep learning architecture has significantly advanced the field of medical image segmentation, particularly for brain tumors. From CNNs and U-Net to 3D CNNs and GANs, each architecture has contributed unique strengths to address the challenges of brain tumor segmentation. However, challenges such as limited labeled data, class imbalance, and variability in imaging protocols remain. Recent advancements in transfer learning, attention mechanisms, and data augmentation have shown promise in overcoming these

challenges, paving the way for more accurate and reliable segmentation methods.

The key contributions of our research can be summarized as follows:

–This research demonstrates the end-to-end training and evaluation of a deep lightweight neural network for brain tumor segmentation using the BraTS2020 dataset. We explored critical data preprocessing techniques, utilized the PatchNet, DeepLab, and FCNN architectures, and employed a full set of evaluation metrics to achieve robust and reliable model performance. Throughout, we emphasized attention to 3D medical image processing, appropriate preprocessing procedures, and the selection of evaluation metrics that provide insight into segmentation quality.
–This study provides a useful basis for future research and potential clinical applications in the medical image segmentation. This accomplishment underscores the promise of deep learning solutions for solving challenging medical image analysis tasks, such as segmenting brain tumors from MRI snapshots.
–This study lays good groundwork for future applications and research in medical image segmentation. A few potential directions to further improve this work are as follows: trying other network structures, e.g., attention networks; hyperparameter optimization for better performance; and using advanced techniques such as data augmentation, transfer learning, or ensemble strategies to further improve segmentation accuracy. Additional improvement may also be realized by leveraging domain knowledge and post-processing techniques to further refine the predictions of the model and its clinical utility.

By building on these efforts, we wish to contribute to the creation of tools that will allow clinicians to diagnose and treat brain tumors more precisely and effectively and thereby improve patient outcomes.

3 Materials and Methodology

In this section, we provide a detailed description of the methodology used to improve brain tumor segmentation using fine-tuned deep learning models and data augmentation techniques. The method is split into several key components: dataset description, records preprocessing, statistics augmentation, model architectures (PatchNet, DeepLab, and FCNN), best tuning, training, and evaluation metrics, as shown in Fig. 1.

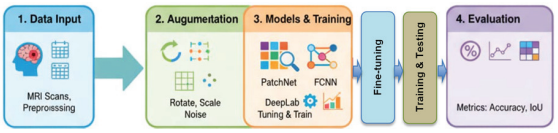

Fig. 1: The methodology

3.1 Dataset Description

The Brain Tumor Segmentation (BraTS) 2020 dataset is a famous and widely used multimodal Magnetic Resonance Imaging (MRI) scan dataset for brain tumor segmentation tasks. The dataset consists of MRI scans of glioma patients, which are brain tumors that occur from glial cells in the brain. Every patient case includes four various MRI modalities, as shown in Fig. 2 and Fig. 3, which include complementary information about brain tissue and tumor characteristics. These modalities are:

–**Native T1-weighted (T1):** This type of imaging offers anatomical details of the brain with high resolution, with emphasis on the structural integrity of tissues. It is extremely helpful in visualizing normal brain anatomy and discriminating between several types of tissues [26].
–**Post-contrast T1-weighted (T1ce - contrast-enhanced):** In this modality, the patient receives a gadolinium-based contrast agent, allowing easier visualization of disturbed blood-brain barrier areas, such as active tumor sites. This modality is useful for the detection of enhancing tumor components [15].
–**T2-weighted (T2):** T2-weighted images are sensitive to fluid and are optimal at detecting regions of edema (fluid) and cystic or necrotic regions in the tumor. This modality is helpful in providing contrast between fluid-containing regions and solid tissues [26].
–**T2-FLAIR (T2-Fluid Attenuated Inversion Recovery):** It suppresses the signal of free fluid (e.g., cerebrospinal fluid) but keeps other tissues' signals intact. It is particularly useful in showing peritumoral edema and non-enhancing tumor regions that are obscured in routine T2-weighted images [15].

Each patient's dataset includes co-registered and skull-stripped volumes in these four modalities for the purpose of spatial registration and multimodal analysis. The dataset also includes expert-annotated segmentation masks that delineate the tumor into individual sub-regions, delineating the heterogeneity of gliomas. The annotations are provided in the form of pixel-wise labels, where each label corresponds to an individual tumor sub-region or non-tumor tissue. The labeling scheme is as follows:

–**Label 0:** Not Tumor (NT): This category encompasses all non-tumor regions in the brain, including normal brain tissue, cerebrospinal fluid, and other non-pathological systems.

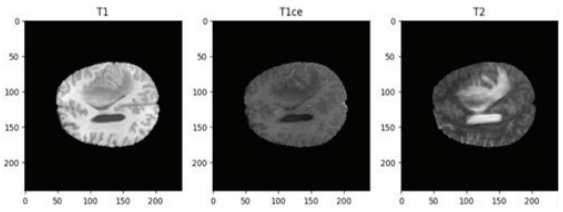

Fig. 2: Different modalities of an MRI image slice number 60 from left to right: T1, T1ce, T2, Flair, and Mask

–**Label 1:** Necrotic and Non-Enhancing Tumor Core (NCR/NET): This label is used to identify the necrotic (dead) tissue in the tumor core and segments of the tumor that do not enhance on contrast. These segments usually equate to less active or non-viable tumor tissue.
–**Label 2:** Peritumoral Edema (ED): This label is used to describe the edematous (swollen) brain tissue surrounding the tumor, typically because of the spillage of fluid out of the tumor into surrounding brain parenchyma. Edema is a common feature of gliomas and can contribute to the overall mass effect of the tumor.
–**Label 3:** Missing: This is reserved for spaces where there isn't a proper annotation. Unsurprisingly, in the case of the BraTS 2020 dataset, no pixels on any of the volumes are labeled with this category, implying all spaces have been annotated [16].
–**Label 4:** GD-Enhancing Tumor (ET): It labels the region in the tumor that enhances after gadolinium contrast administration. It usually describes active, high-grade regions of tumor with blood-brain barrier disruption.

The BraTS 2020 data set is a valuable resource for developing and evaluating automated brain tumor segmentation algorithms because it provides a well-annotated and standardized multimodal MRI data set. Having multiple MRI modalities and extensive annotations allows researchers to study the complex spatial and structural heterogeneity of gliomas, which is crucial for accurate diagnosis, treatment planning, and follow-up of brain tumor patients [15], [26].

3.2 Data Preprocessing

Preprocessing is a critical step to ensure the quality and consistency of the input data. The following preprocessing steps were applied:

–**Skull Stripping:** Non-brain tissues were removed using the Brain Extraction Tool (BET) from the FSL software suite. This step ensures that the model focuses only on brain regions [19].

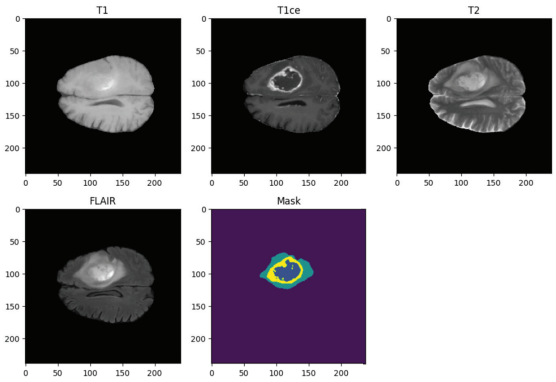

Fig. 3: Different modalities of an MRI image slice number 95 from left to right: T1, T1ce, T2, Flair, and Mask

–**Normalization:** Intensity values were normalized to the range $[0, 1]$ using min-max normalization:

$$I_{norm} = \frac{I - I_{min}}{I_{max} - I_{min}} \tag{1}$$

where I is the original intensity value, and I_{min} and I_{max} are the minimum and maximum intensity values in the volume [**?**].
–**Co-registration:** All MRI modalities (T1, T1c, T2, FLAIR) were co-registered to the same spatial space to ensure alignment. This step is crucial for multi-modal fusion [21].
–**Patch Extraction:** For PatchNet, the input volumes were divided into smaller patches of size $64 \times 64 \times 64$ voxels. This reduces memory requirements and allows the model to focus on local features [6].

3.3 Data Augmentation

Data augmentation is essential to increase the diversity of the training dataset and improve model generalization. The following augmentation techniques were applied:

1.**Rotation:** Randomly rotating images by angles between $-15°$ and $15°$.
2.**Flip:** Horizontally and vertically flipping images.
3.**Scaling:** Randomly scaling images by factors between 0.9 and 1.1.
4.**Translation:** Shifting images by up to 10% of their width and height.
5.**Elastic Deformations:** Applying small elastic deformations to simulate natural variations in brain anatomy.

These transformations were applied on-the-fly during training to generate new training samples dynamically [22], [23], [24].

4 Model Architectures

We evaluated three model architectures: PatchNet, DeepLab, and the proposed model (Fast Convolutional Neural Network (FCNN)). Each model was fine-tuned using transfer learning and trained with data augmentation.

4.1 PatchNet

In order to concentrate on localized features, the PatchNet architecture first splits the input image into small, overlapping or non-overlapping patches. Each patch is then analyzed independently. A convolutional neural network (CNN) is then used to treat these individual patches, which removes important properties without considering the global structure of the total image [23]. After patchwork processing, the properties obtained from each patch are collected or integrated using more complex fusion techniques to generate a full representation of the image. To produce the final prediction, which could require class labeling or region segmentation, this aggregated feature set is further passed via fully connected layers or other classification/segmentation components, as shown in Fig. 4.

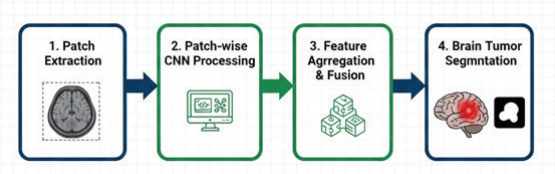

Fig. 4: PatchNet architecture process

4.2 DeepLab

DeepLab uses atrous (dilated) convolutions to capture multi-scale features and a CRF to refine segmentation boundaries [25]. The architecture is shown in Fig. 5. DeepLab architecture for semantic segmentation begins with feature extraction utilizing a backbone network like MobileNet, ResNet, or Xception. These networks, often pretrained on large datasets such as ImageNet, are adapted to maintain high spatial resolution through the use of dilated convolutions. Instead of standard convolutions, DeepLab later replaced layers to expand the receptive area without reducing the feature map solution so that the model can occupy more global context and multiscale without increasing the number of parameters. To improve multiscale feature learning, DeepLab introduces atrous spatial pyramid pooling (ASPP), where several parallel atrous convolutions are used with different dilation rates, catching objects and patterns on different scales. The outputs from these branches are then combined to create a rich representation on several levels. A simple 1×1 conversion is used on the ASPP output to generate a coarse segmentation map, which predicts class probabilities on each pixel.

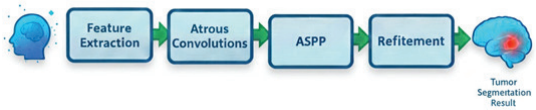

Fig. 5: DeepLab architecture process

4.3 The proposed model: Fast Convolutional Neural Network (FCNN)

This section introduces the lightweight FCNN, a unique deep learning model created especially for enhanced brain tumor segmentation. This model's goal is to provide a compromise between low computational complexity and good detection accuracy, which makes it suitable for quick scientific diagnoses. As seen in Fig. 6, the FCNN architectural design. Our inference framework employs a more flexible design with fewer layers and filters than the convolutional neural network (CNN) architecture, which is typically demanding and processing costly. We limit the amount of parameters and concentrate on improving performance in feature extraction and classification. This approach makes the model appropriate for real-time applications while lowering the amount of time and computing resources needed for training.

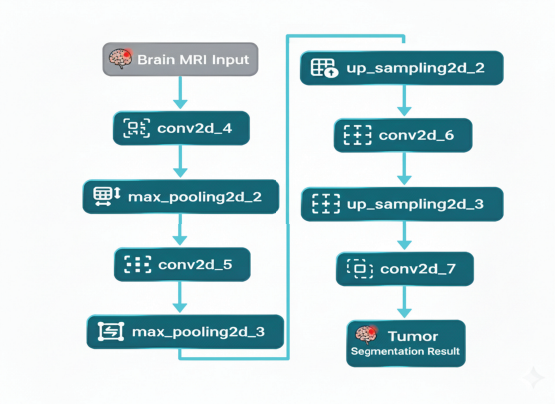

Fig. 6: Architecture of the Fully Convolutional Neural Network (FCNN)

Table 1 showcases the details of a compact Fast Convolutional Neural Network (FCNN) architecture

designed for efficiency. The model kicks off with a conv2D layer that transforms the input into a feature map of dimensions (128, 128, 32), utilizing 608 parameters. This is observed by way of a maxpooling2D layer that compresses the feature map to (64, 64, 32) without introducing any additional parameters. Next, a second conv2D layer processes the data with 9,248 parameters, after which another pooling layer reduces the spatial dimensions to (32, 32, 32). Transitioning into the decoding phase, the model employs an Upsampling2D layer to restore the size back to (64, 64, 32). It then uses another convolutional layer that mirrors the previous one, also with 9,248 parameters. This is succeeded by using any other up-sampling layer that brings the resolution back to the original size of (128, 128, 32). Finally, the output conv2D layer refines the data using 132 parameters, producing an intensity of four channels appropriate for multi-class segmentation tasks. In general, the model consists of 19,236 parameters (approximately 75.14 kb), all of which are trainable, making it an effective and compact solution ideal for settings with limited computational resources.

Table 1: Architecture of the proposed FCNN model

Layer (type)	Output Shape	Param #
conv2d_4 (Conv2D)	(None, 128, 128, 32)	608
max_pooling2d_2 (MaxPooling2D)	(None, 64, 64, 32)	0
conv2d_5 (Conv2D)	(None, 64, 64, 32)	9,248
max_pooling2d_3 (MaxPooling2D)	(None, 32, 32, 32)	0
up_sampling2d_2 (Upsampling2D)	(None, 64, 64, 32)	0
conv2d_6 (Conv2D)	(None, 64, 64, 32)	9,248
up_sampling2d_3 (Upsampling2D)	(None, 128, 128, 32)	0
conv2d_7 (Conv2D)	(None, 128, 128, 4)	132
Total params: 19,236 (75.14 KB) Trainable params: 19,236 (75.14 KB) Non-trainable params: 0 (0.00 B)		

Fine-Tuning: Fine-tuning involves adjusting the parameters of pre-trained models to adapt them to the brain tumor segmentation task. The learning rate for the encoder was set lower than that of the decoder to preserve the learned features. The fine-tuning process can be described as:

$$\theta_{final} = \theta_{pre-trained} + \Delta\theta \tag{2}$$

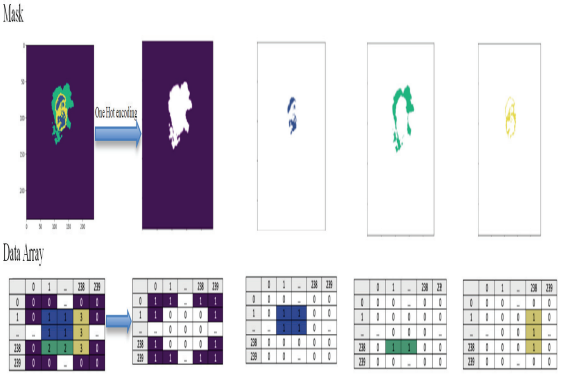

Fig. 7: One-hot encoding

where $\theta_{pre-trained}$ represents the pre-trained weights, and $\Delta\theta$ represents the adjustments made all through fine-tuning [29].

Training: The models have been trained using the Dice loss function, which is well-suited for segmentation tasks due to its capacity to handle class imbalance. The Dice loss is described as

$$Dice\ Loss = 1 - \frac{2\sum_i p_i g_i}{\sum_i p_i + \sum_i g_i} \tag{3}$$

where p_i represents the predicted segmentation mask, and g_i represents the ground truth mask. We used the Adam optimizer with a batch size of 16 and trained the models for 10 epochs. A learning rate scheduler was employed to adjust the learning rate during training, starting with a higher rate and gradually reducing it. Early stopping was used to prevent overfitting [30].

5 The Proposed Approach

We described our proposed approach using the following two algorithms. **Algorithm 1** outlines the structure and operation of a custom data generator designed for MRI image segmentation.

Image resize: Resize every slice from (1240x1240) to (128x128) becoming properly in PatchNet and FCNN networks and (256x256) becoming properly in DeepLab network. This form is chosen because it is a power of two, and balances computational efficiency and preserved information.

One hot encoding: It applies to the mask array to convert classes (0 to 3) into formatting of numerical suitable for neural networks, as shown in Fig. 7.

This DataGenerator is an efficient manner to load, preprocess, and feed big-scale MRI segmentation facts to a deep learning model without strolling into reminiscence constraints. It guarantees proper facts, pipeline glide, handling of missing files, and cleaning of segmentation labels, making it best for schooling a brain tumor

Algorithm 1 DataGenerator for MRI Image Segmentation

Require: **list_IDs:** List of image identifiers
Require: **Dim:** Target image dimensions (height, width)
Require: **Batch_size:** Number of samples per batch
Require: **Shuffle:** Boolean flag for shuffling data
Ensure: Batch of preprocessed MRI images X and one-hot encoded segmentation masks y.
Step 1: Initialization (init)
Accept list_IDs, dim, batch_size, and shuffle as input parameters.
Initialize internal attributes.
Call on_epoch_end().
Step 2: Define Number of Batches (len)
$num\_batches = \lfloor total\_samples/batch\_size \rfloor$
Step 3: Fetch a Batch (getitem)
Select batch indices.
Retrieve corresponding image IDs.
Generate batch data.
Return (X, y).
Step 4: Shuffle Data (on_epoch_end)
Generate index array.
Shuffle if enabled.
Step 5: Data Generation
Initialize X and y.
For each image ID:
Load FLAIR and T1ce images.
Load segmentation mask.
Remove invalid labels.
Resize images and masks.
Normalize intensities.
Apply one-hot encoding.
Step 6: Output
Return (X, y).

segmentation version on the usage of deep mastering. **Algorithm 2** gives a description of the fine-tuning process of an FCNN for the function of brain tumor sharing into 2 multimodal MRI images. Tuning is performed using random searches in the cause, which enables automated exploration of different model architectures and training configurations to adapt the performance. This process begins with defining an FCNN-based partition model that accepts entrance images of 128×128 with two channels, and T1CE represents MRI methods. Model architecture has a coder-based structure, which has conventions and merger layers for functional extraction and discharge, followed by upsampling layers to organize the spatial resolution of the partition output. The final layer uses a Softmax activation feature with four filters so that the model can divide the pixel multi-class according to four different physical or disease areas. The Adam Optimizer is chosen for training due to its adaptive learning ability, with a predetermined set $\{10^{-2}, 10^{-3}, 10^{-4}\}$. The tuning process is carried out using a random discovery algorithm as a random configuration within the defined hyperparameter room. This method allows for the automatic choice of the greatest network intensity, feature dimensionality, and learning rate, which appreciably influence the accuracy and generalization functionality of segmentation models in medical imaging responsibilities.

Algorithm 2 Fine-Tuning FCNN for Brain Tumor Segmentation Using Keras

Require: MRI image size patch (128, 128, 2)
Require: Partition mask with 4 square meters
Require: Search placement for number of filters and learning frequency.
Ensure: FCNN model set up with custom hyperparameters
Step 1: Define FCNN model
Define input shape as (128, 128, 2) to simply accept twin-modality MRI snapshots.
Add a Conv2D layer with filters $\in \{32, 64, 128\}$ (chosen using hp.Choice()), kernel size = 3, activation = ReLU.
Add a **MaxPooling2D** layer to reduce spatial dimensions.
Add a **2D Conv2D** layer with tunable filter size, identical as in Step 1.2.
Add a second MaxPooling2D layer.
Add an **UpSampling2D** layer to repair spatial resolution.
Add a second UpSampling2D layer.
Add a final **Conv2D** layer with four filters and softmax activation for pixel-sensible category into 4 instructions.
Compile the model using of the Adam optimizer by getting a rate $\in \{1e-2, 1e-3, 1e-4\}$.
Step 2: Set the Hyperparameter Tuner
Initialize a RandomSearch tuner with the following settings:
• Objective: "Val_accuracy"
• Maximum test: 2
• directory and project name to save search results
Define the search area:
1. Number of filters in conv2D -layer
2. Learning Frequency for Optimizer
Provide training and verification data through training generators and valid_generators.
Step 3: Perform Hyperparameter Search
Start search using the search with tuner.search():
• Training data
• Validation data
• The number of epochs.
• batch size
Tuner evaluates different combinations and records the performance measurements.
Step 4: Retrieve and Use the Best Model
Receive the best hyperparameter using tuner.get_best_hyperparameter()
Rebuild the model using tuner.hypermodel.build (best_hps).
Evaluate and train the final model data sets.

The tuning process begins with the definition of an FCNN architecture that accepts input images of size 128×128 with two channels, representing the multimodal MRI inputs (FLAIR and T1CE). The model follows an encoder-decoder structure, where the encoder extracts features through convolutional and pooling

layers, and the decoder restores spatial resolution through upsampling layers. The final convolutional layer uses a softmax activation function with four filters to perform multi-class segmentation into four different tissue regions. The Adam optimizer is employed for training, with learning rates selected from $\{10^{-2}, 10^{-3}, 10^{-4}\}$ through the hyperparameter tuning process.

6 Evaluation Metrics

To thoroughly assess how well a brain tumor segmentation model performs, we utilize a detailed array of metrics. These metrics shed light on the model's effectiveness in accurately outlining tumor sub-regions while tackling the difficulties posed by imbalanced datasets, exemplified by the BraTS 2020 dataset, where the volume is largely comprised of non-tumor regions (background). Below, we will mathematically define these metrics and explore their importance in the realm of brain tumor segmentation.

Accuracy: it quantifies the overall proportion of correctly classified pixels in the segmentation output and is defined as:

$$Accuracy = \frac{TP + TN}{TP + TN + FP + FN} \tag{4}$$

where TP, TN, FP, and FN denote true positives, true negatives, false positives, and false negatives, respectively. Although accuracy is a straightforward metric, it can be misleading when applied to imbalanced datasets where one class (such as background) significantly outnumbers the others. In the context of brain tumor segmentation, high accuracy scores may not adequately represent the model's proficiency in accurately segmenting small or rare tumor sub-regions [16].

Intersection over Union (IoU): it is commonly referred to as the Jaccard Index and quantifies the overlap between the predicted segmentation and the ground truth. It is defined as follows:

$$IOU = \frac{TP}{TP + FP + FN} \tag{5}$$

where TP represents true positives, FP denotes false positive, and FN signifies false negative. The IoU score ranges from 0, indicating no overlap, to 1, indicating perfect overlap. It is specifically touchy to each false positives and false negatives, making it a valuable metric for assessing the spatial agreement between the model's predictions and expert annotations [26].

Dice Coefficient: commonly referred to as the F1 score, it assesses the similarity between predicted and ground truth segmentations. It is defined as follows:

$$Dice = \frac{2 \times TP}{2 \times TP + FP + FN} \tag{6}$$

The Dice Coefficient is considerably applied in medical photo segmentation because of its robustness in handling class imbalances and its ability to provide a balanced evaluation of segmentation performance. Like the IoU, it ranges from 0 to 1, with higher values signifying superior overall performance [16].

Sensitivity, also known as Recall or True Positive Rate, quantifies the proportion of positive ground truth pixels, such as tumor regions, that the model accurately predicts as positive. It is defined as follows:

$$Sensitivity = \frac{TP}{TP + FN} \tag{7}$$

A high sensitivity value signifies that the model is proficient in identifying tumor regions, which is essential for clinical applications where the oversight of tumor tissue may lead to significant repercussions [26].

Precision, additionally referred to as Positive Predictive Value, assesses the ratio of predicted positive pixels that correspond to true positive values in the ground truth. It is calculated using the subsequent formulation:

$$Precision = \frac{TP}{TP + FP} \tag{8}$$

A high precision value means that the model effectively reduces false positives, that's critical for minimizing over-segmentation and suring the accuracy of predicted tumor regions [15].

Specificity: Specificity, also known as the True Negative Rate, quantifies the proportion of negative ground truth pixels (such as non-tumor regions) that the model, as it should be predicted as negative. It is defined by the formulation:

$$Specificity = \frac{TN}{TN + FP} \tag{9}$$

While specificity may be less critical in tumor segmentation compared to sensitivity and precision, it offers valuable insights into the model's capability to correctly identify healthy tissue [26].

7 Results and Discussion

This research examines how hyperparameter tuning and data augmentation influence the performance of deep learning models in brain tumor segmentation. We compare our suggested method FCNN with established models like PatchNet, and DeepLab to measure enhancements in segmentation precision and model generalization. Through the careful integration of precisely calibrated model architectures with a variety of enhanced training data, our approach provides a more reliable and precise solution for brain tumor segmentation, aiding clinicians in making more accurate diagnostic and therapeutic choices.

Fig. 8 shows training against verification accuracy (left) and training vs. verification loss (right) using the FCNN model. These plots show the models' learning

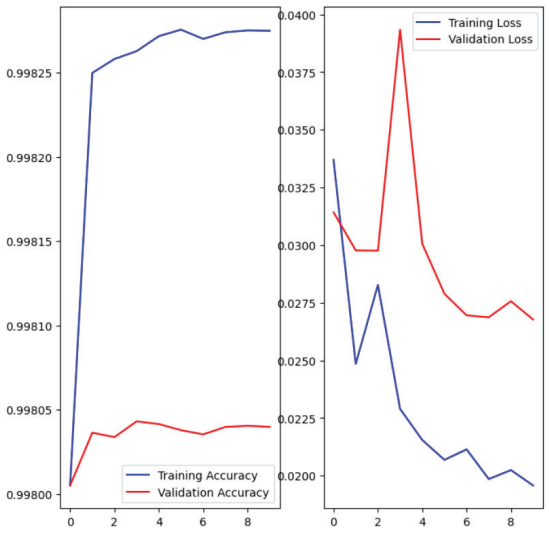

Fig. 8: The accuracy and loss of training and validation performance of a FCNN deep learning model over 10 epochs

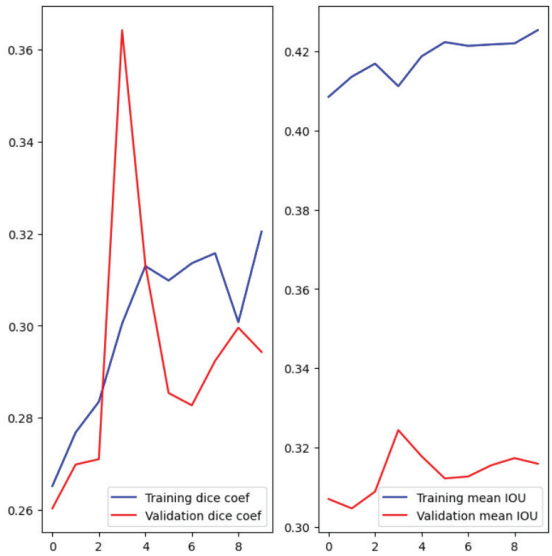

Fig. 9: The Dice coefficient and mean Intersection over Union (IoU) the performance matrices of FCNN model

behavior and performance through the training process. The curves indicate that the model acquires high accuracy with minimum losses and reflects strong convergence and effective generalization. The narrow gap between exercise and verification measurements suggests that the model is well trained, with a low margin of minimal overdue and fault. Overall, the results suggest that the FCNN model provides a segmentation performance in the Brats2020 validation setting.

Fig. 9 presents the segmentation performance metrics of the FCNN model over 10 training epochs. The left plot shows the Dice coefficient, a commonly used metric for evaluating the overlap among predicted and ground truth segmentation masks. The Dice coefficient exhibits a consistent upward trend throughout training, indicating progressive improvement in the model's learning functionality. The right plot shows the Mean IoU, another overlap-based metric that is particularly sensitive to false positives. The IoU demonstrates a stable and gradual increase across epochs, in our evaluation, the proposed method received a high performance metrics than selected techniques under specific conditions with the Brats2020 dataset.

A qualitative outcome of our strategy from the validation subsets is shown in Fig. 10. The proposed method successfully segmented the tumor regions in most validation cases, particularly when boundaries were well-defined, and the images that do not contain the tumor also perform well (no segmentation in the prediction images). Furthermore, the core tumor has been satisfactorily segmented. Certain visuals work well for visualization, while others don't. Lastly, a large number of early tumor photos lack appropriate segmentation. We have a goal for future work to improve this last kind of tumor.

The per-class Dice coefficient functions are used to evaluate the segmentation performance of a model by calculating the Dice coefficient for specific tumor regions. These functions help in accurately measuring how well the model predicts different parts of the tumor. The dice_coef_necrotic function calculates the Dice coefficient for the necrotic (dead tissue) region of the tumor by computing the intersection over the sum of squares of the true and predicted values for the necrotic class. Similarly, the dice_coef_edema function measures the cube coefficient for the edema (swelling) region, evaluating how accurately the model captures this area. Lastly, the dice_coef_enhancing characteristic calculates the dice coefficient for the enhancing tumor region, focusing on the parts of the tumor that display contrast enhancement. Together, these functions provide detailed insights into the model's ability to segment and differentiate between various tumor structures.

Table 2 presents a comparative assessment of three partition models - FCNN, Patchnet and DeepLab - More performance measurements. Among them, the FCNN model shows the best total performance, the lowest loss (0.0303) and the highest accuracy (0.9981). In addition, FCNN receives the highest intersection and dice coefficients of 0.2526 at Intersection over Union (IoU) at 0.3168, reflecting a more overlap between the approximate division and the ground. The PatchNet model ranks second, where it shows competitive results in accuracy (0.9817), and sensitivity (0.9812). These calculations suggest that PatchNet performs well and normalize es well, although it does not match the level of

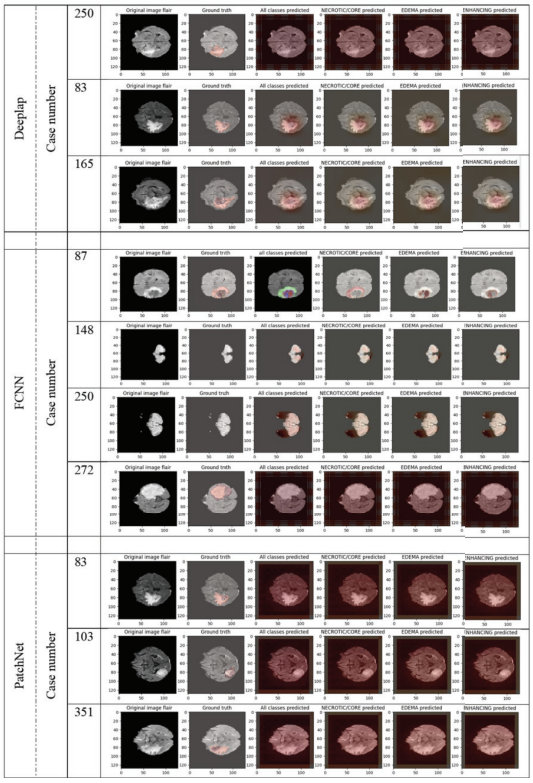

Fig. 10: Qualitative results obtained from the validation subset of the BraTS 2020 training dataset. From left to right: original image flair, ground truth, all classes predicted, necrotic/core, edema, and enhancing predicted

consistency and accuracy of FCNN. In contrast, the DeepLab model shows the weakest performance in almost all considered matrix. It reports the highest loss (0.3709) and the lowest accuracy (0.8165). While sensitivity remains relatively high (0.9499), indicating the right ability to identify proper positivity, its accuracy and specificity are low, suggesting a higher rate of false positivity.

In addition, Deeplab specifically shows the lower class-specific dice score, especially to challenge tumor subgroups such as necrotic tissue (0.0204) and to increase the tumor (0.0168), indicates difficult ties in fragmenting small or less specific areas. In summary, FCNN appears as the most consistent and accurate model for brain tumor segmentation among between the three models, followed by the PatchNet, which provides the right performance. DeepLab lags behind in both overall and class-specific segmentation.

Compared with state-of-art methods: Table 3 presents a comparative analysis of the performance of the proposed technique against several existing methods for brain tumor segmentation, focusing on their accuracy. Traditional clustering methods, like k-means combined

Table 2: Quantitative evaluation of DeepLab, FCNN, and PatchNet models

Metric	DeepLab	FCNN	PatchNet
Loss	0.3709	**0.0303**	0.1262
Accuracy	0.8165	**0.9981**	0.9817
Mean IoU	0.1820	**0.3168**	0.2500
Dice coefficient	0.2238	**0.2526**	0.2346
Precision	0.7960	**0.9982**	0.9813
Sensitivity	0.9499	**0.9958**	0.9812
Specificity	0.7947	**0.9994**	0.9939
Class-wise Dice coefficients:			
Necrotic	0.0204	0.0026	0.0176
Edema	0.0509	0.0157	0.0272
Enhancing	0.0168	0.0103	0.0140

with FCM [31], and bisecting methods [30], demonstrated limitations in handling complex medical imaging, achieving only 56.40% and 83.05% accuracy, respectively. In contrast, deep learning techniques yielded significantly better outcomes. For instance, the original U-NET architecture [4] achieved an impressive 92.0% accuracy on the Brats2020 dataset. Variants like U-NET-VGG16 [33] and VGG-19 with decoders [32] showed even greater improvements, reaching 96.10% and 97.26% accuracy, respectively. More sophisticated architectures, such as 3Encoder with decoder [32] and its updated BiFPN [32] version, attained an accuracy of 99.10%. Recent techniques like RES-UNeT [34] and FTVT-L16 [35] have additionally shown strong overall performance, delivering accuracies of 97.95% and 98.70%, respectively. Notably, a fully Convolutional Network (FCN) model executed a high accuracy of 99.1% at the TCGA dataset [36]. Ultimately, the delivered method outperformed all the listed techniques, reaching an incredible accuracy of 99.81% at the Brats2020 dataset, underscoring its advanced functionality in accurately segmenting brain tumors.

The limitations of our work: Despite promising results, this study has many limitations. First, the experiments were limited to the BraTS2020 dataset, limiting the model's generalization to other datasets or clinical environments. Second, the method relies on manually annotated training data, which cannot fully capture the variability of tumor morphology in different populations. Third, while fine-tuning and improvements improved the model's accuracy, they also increased the computational cost and training time. Finally, further validation with independent datasets and prospective clinical data is required to confirm robustness and applicability in actual clinical workflows.

Table 3: Comparison of the suggested model's performance with recent methods

Method	Database	Accuracy (%)
Bisecting (no initialization) [30]	MRI collected by authors	83.05
K-means and FCM [31]	Radiopaedia.org	56.40
U-Net [4]	BraTS2020	92.00
U-Net-VGG16 [33]	Data approved by Dr. Soetomo Surabaya	96.10
VGG-19 + Decoder [32]	BraTS2020	97.26
3Encoder + Decoder [32]	BraTS2020	98.29
3Encoder + BiFPN + Decoder [32]	BraTS2020	98.99
3Encoder + BiFPN + AttDecoder [32]	BraTS2020	99.10
Res-UNet [34]	BraTS2020	97.95
FTVT-L16 [35]	Figshare, SARTAJ, and Br35H	98.70
FCN [36]	TCGA	99.10
Our method	**BraTS2020**	**99.81**

8 Conclusion

The proposed fine-tuned full convolutional neural network (FCNN) demonstrated high segmentation accuracy and strong generalization ability in automatic brain tumor detection from MRI data. Quantitative evaluation on the BraTS2020 dataset showed that FCNN achieved an accuracy of 0.9981, an average IoU of 0.3168, and a Dice coefficient of 0.2526, outperforming DeepLab and PatchNet under the same experimental settings. The model also achieved accuracy (0.9982), sensitivity (0.9958), and specificity (0.9994), confirming its reliability in accurately distinguishing tumor and non-tumor regions with minimal misidentification.

Although these global metrics are encouraging, class-specific DICE scores–necrotic (0.0026), edema (0.0157), and growth (0.0103)–indicate that improved tumor subregion segmentation remains challenging. These findings reflect the limitations of two-dimensional modeling and class imbalance in the data set, suggesting that better spatial context and balanced data augmentation are needed.

The observed results validate the effectiveness of the proposed fine-tuning and enhancement strategy, which optimized learning stability while maintaining a lightweight, computationally efficient design suitable for clinical deployment. Future research will extend the model towards 3D volumetric architectures, attentional or transformer-based modules, and semi-supervised or domain-adaptive techniques to increase generalization and reduce annotation dependency. Comparative evaluation with recent segmentation approaches further supports the strength of the proposed model: it achieved an accuracy of 99.81% on the BraTS2020 dataset, outperforming U-Net (92.0%), Res-UNet (97.95%) and FTVT-116 (98.70%). This highlights the efficiency, accuracy, and reliability of the proposed FCNN as a promising framework for high-precision brain tumor segmentation.

In conclusion, the proposed fine-tuned FCNN provides a robust, interpretable and computationally efficient framework for brain tumor segmentation, achieving a scientifically sound balance between accuracy and complexity. This establishes a promising direction for the development of next-generation, clinically deployable deep learning systems in neuro-oncology imaging.

Future work: The use of semi-supervised and unsupervised learning techniques may be explored in order to lessen reliance on extensive labeled datasets, which are frequently hard to come by in the medical domain. Future research should evaluate the suggested approach's practical application by validating it in actual clinical settings.

Conflicts of Interest: The authors have no conflicts of interest.

Data Availability Statement: The data used in this study are publicly available from the Kaggle BraTS2020 dataset. Access is provided via: https://www.kaggle.com/datasets/awsaf49/brats20-dataset-training-validation (accessed on 1 January)

References

[1] Bauer, S., Wiest, R., Nolte, L. P., & Reyes, M. (2013). A survey of MRI-based medical image analysis for brain tumor studies. *Physics in Medicine and Biology*, 58(13), R97–R129.

[2] Menze, B. H., Jakab, A., Bauer, S., Kalpathy-Cramer, J., Farahani, K., Kirby, J., & Van Leemput, K. (2015). The multimodal brain tumor image segmentation benchmark (BRATS). *IEEE Transactions on Medical Imaging*, 34(10), 1993–2024.

[3] Litjens, G., Kooi, T., Bejnordi, B. E., Setio, A. A. A., Ciompi, F., Ghafoorian, M., & van Ginneken, B. (2017). A survey on deep learning in medical image analysis. *Medical Image Analysis*, 42, 60–88.

[4] Ronneberger, O., Fischer, P., & Brox, T. (2015). U-Net: Convolutional networks for biomedical image segmentation. In *International Conference on Medical Image Computing and Computer-Assisted Intervention* (pp. 234–241). Springer, Cham.

[5] Isensee, F., Jaeger, P. F., Kohl, S. A., Petersen, J., & Maier-Hein, K. H. (2021). nnU-Net: A self-configuring method for deep learning-based biomedical image segmentation. *Nature Methods*, 18(2), 203–211.

[6] Kamnitsas, K., Ledig, C., Newcombe, V. F., Simpson, J. P., Kane, A. D., Menon, D. K., & Glocker, B. (2017). Efficient multi-scale 3D CNN with fully connected CRF for accurate brain lesion segmentation. *Medical Image Analysis*, 36, 61–78.

[7] Havaei, M., Davy, A., Warde-Farley, D., Biard, A., Courville, A., Bengio, Y., & Larochelle, H. (2017). Brain tumor segmentation with deep neural networks. *Medical Image Analysis*, 35, 18–31.

[8] Perez, L., & Wang, J. (2017). The effectiveness of data augmentation in image classification using deep learning. *arXiv preprint arXiv:1712.04621*.

[9] Bergstra, J., & Bengio, Y. (2012). Random search for hyper-parameter optimization. *Journal of Machine Learning Research*, 13(2), 281–305.

[10] Long, J., Shelhamer, E., & Darrell, T. (2015). Fully convolutional networks for semantic segmentation. In *Proceedings of the IEEE Conference on Computer Vision and Pattern Recognition* (pp. 3431–3440).

[11] Chen, L. C., Papandreou, G., Kokkinos, I., Murphy, K., & Yuille, A. L. (2017). DeepLab: Semantic image segmentation with deep convolutional nets, atrous convolution, and fully connected CRFs. *IEEE Transactions on Pattern Analysis and Machine Intelligence*, 40(4), 834–848.

[12] Zhao, X., Wu, Y., Song, G., Li, Z., Zhang, Y., & Fan, Y. (2018). A deep learning model integrating FCNNs and CRFs for brain tumor segmentation. *Medical Image Analysis*, 43, 98–111.

[13] Oktay, O., Schlemper, J., Le Folgoc, L., Lee, M., Heinrich, M., Misawa, K., ... & Glocker, B. (2018). Attention U-Net: Learning where to look for the pancreas. *arXiv preprint arXiv:1804.03999*.

[14] Xue, Y., Xu, T., Zhang, H., Long, L. R., & Huang, X. (2018). SegAN: Adversarial network with multi-scale L1 loss for medical image segmentation. *Neuroinformatics*, 16(3-4), 383–392.

[15] Bakas, S., Akbari, H., Sotiras, A., Bilello, M., Rozycki, M., Kirby, J. S., ... & Davatzikos, C. (2017). Advancing the cancer genome atlas glioma MRI collections with expert segmentation labels and radiomic features. *Scientific Data*, 4(1), 1-13.

[16] Bakas, S., Reyes, M., Jakab, A., Bauer, S., Rempfler, M., Crimi, A., ... & Menze, B. (2018). Identifying the best machine learning algorithms for brain tumor segmentation, progression assessment, and overall survival prediction in the BRATS challenge.

[17] Çiçek, Ö., Abdulkadir, A., Lienkamp, S. S., Brox, T., & Ronneberger, O. (2016). 3D U-Net: Learning dense volumetric segmentation from sparse annotation. In *Medical Image Computing and Computer-Assisted Intervention – MICCAI 2016* (pp. 424–432). Springer.

[18] Taha, A. A., & Hanbury, A. (2015). Metrics for evaluating 3D medical image segmentation: analysis, selection, and tool. *BMC Medical Imaging*, 15(1), 29.

[19] Smith, S. M. (2002). Fast robust automated brain extraction. *Human Brain Mapping*, 17(3), 143–155.

[20] Nyúl, L. G., Udupa, J. K., & Zhang, X. (2000). New variants of a method of MRI scale standardization. *IEEE transactions on medical imaging*, 19(2), 143-150.

[21] Jenkinson, M., Bannister, P., Brady, M., & Smith, S. (2002). Improved optimization for the robust and accurate linear registration and motion correction of brain images. *NeuroImage*, 17(2), 825–841

[22] Shorten, C., & Khoshgoftaar, T. M. (2019). A survey on image data augmentation for deep learning. *Journal of Big Data*, 6, 60.

[23] Simard, P. Y., Steinkraus, D., & Platt, J. C. (2003). Best practices for convolutional neural networks applied to visual document analysis. In *Proceedings of the International Conference on Document Analysis and Recognition* (pp. 958–963).

[24] Zeineldin, R. A., & Mathis-Ullrich, F. (2024). Unified HT-CNNs architecture: Transfer learning for segmenting diverse brain tumors in MRI from gliomas to pediatric tumors. *arXiv preprint arXiv:2412.08240*. https://arxiv.org/abs/2412.08240

[25] Chen, L. C., Papandreou, G., Kokkinos, I., Murphy, K., & Yuille, A. L. (2017). DeepLab: Semantic image segmentation with deep convolutional nets, atrous convolution, and fully connected CRFs. *IEEE Transactions on Pattern Analysis and Machine Intelligence*, 40(4), 834–848. https://doi.org/10.1109/TPAMI.2017.2699184

[26] Menze, B. H., Jakab, A., Bauer, S., Kalpathy-Cramer, J., Farahani, K., Kirby, J., ... & Van Leemput, K. (2015). The multimodal brain tumor image segmentation benchmark (BRATS). *IEEE Transactions on Medical Imaging*, 34(10), 1993–2024. https://doi.org/10.1109/TMI.2014.2377694

[27] Zhao, X., Wu, Y., Song, G., Li, Z., Zhang, Y., & Fan, Y. (2018). A deep learning model integrating FCNNs and CRFs for brain tumor segmentation. *Medical Image Analysis*, 43, 98–111. https://doi.org/10.1016/j.media.2017.10.002

[28] Yosinski, J., Clune, J., Bengio, Y., & Lipson, H. (2014). How transferable are features in deep neural networks?. *Advances in neural information processing systems*, 27.

[29] Isensee, F., Kickingereder, P., Wick, W., Bendszus, M., & Maier-Hein, K. H. (2018). Brain tumor segmentation and radiomics survival prediction: Contribution to the brats 2017 challenge. In *Brainlesion: Glioma, Multiple Sclerosis, Stroke and Traumatic Brain Injuries: Third International Workshop, BrainLes 2017, Held in Conjunction with MICCAI 2017, Quebec City, QC, Canada, September 14, 2017, Revised Selected Papers 3* (pp. 287-297). Springer International Publishing.

[30] Mahmud, M.R.; Mamun, M.A.; Hossain, M.A.; Uddin, M.P. Comparative Analysis of K-Means and Bisecting K-Means Algorithms for Brain Tumor Detection. In *Proceedings of the 2018 International Conference on Computer, Communication, Chemical, Material and Electronic Engineering (IC4ME2)*, Rajshahi, Bangladesh, 8–9 February 2018.

[31] Almahfud, M.A.; Setyawan, R.; Sari, C.A.; Rachmawanto, E.H. An effective MRI brain image segmentation using joint clustering (K-Means and Fuzzy C-Means). In *Proceedings of the 2018 International Seminar on Research of Information Technology and Intelligent Systems (ISRITI)*, Yogyakarta, Indonesia, 21–22 November 2018; IEEE: New York, NY, USA, 2018.

[32] Aboussaleh, I., Riffi, J., Fazazy, K. E., Mahraz, M. A., & Tairi, H. (2023). Efficient U-Net architecture with multiple

encoders and attention mechanism decoders for brain tumor segmentation. *Diagnostics*, 13(5), 872.
[33] Pravitasari, A.A.; Iriawan, N.; Almuhayar, M.; Azmi, T.; Irhamah, I.; Fithriasari, K.; Purnami, S.W.; Ferriastuti, W. UNet-VGG16 with transfer learning for MRI-based brain tumor segmentation. *TELKOMNIKA (Telecommun. Comput. Electron. Control.)* 2020, 18, 1310–1318.
[34] Yu, W., & Wu, G. (2024, November). Enhanced Deep Brain Tumor Segmentation with Medical Image Signal of MRI. In *2024 Cross Strait Radio Science and Wireless Technology Conference (CSRSWTC)* (pp. 1-3). IEEE.
[35] Reddy, C. K. K., Reddy, P. A., Janapati, H., Assiri, B., Shuaib, M., Alam, S., & Sheneamer, A. (2024). A fine-tuned vision transformer based enhanced multi-class brain tumor classification using MRI scan imagery. *Frontiers in oncology*, 14, 1400341.
[36] Sun, H., Yang, S., Chen, L., Liao, P., Liu, X., Liu, Y., & Wang, N. (2023). Brain tumor image segmentation based on improved FPN. *BMC*.
[37] Asiri, A. A., Shaf, A., Ali, T., Shakeel, U., Irfan, M., Mehdar, K. M., Halawani, H. T., Alghamdi, A. H., Alshamrani, A. F. A., & Alqhtani, S. M. (2023). Exploring the power of deep learning: Fine-tuned vision transformer for accurate and efficient brain tumor detection in MRI scans. *Diagnostics*, 13(12), 2094. https://doi.org/10.3390/diagnostics13122094
[38] Ferreira, A., Solak, N., Li, J., Dammann, P., Kleesiek, J., Alves, V., & Egger, J. (2024). How we won BraTS 2023 Adult Glioma challenge? Just faking it! Enhanced synthetic data augmentation and model ensemble for brain tumour segmentation. *arXiv preprint arXiv:2402.17317*. https://arxiv.org/abs/2402.17317
[39] Wang, Y., Ji, Y., & Xiao, H. (2022). A data augmentation method for fully automatic brain tumor segmentation. *arXiv preprint arXiv:2202.06344*. https://arxiv.org/abs/2202.06344

Hanan H. Amin received the B.Sc. degree in Computer Science from Sohag University, Egypt, in 2006, and the M.Sc. and Ph.D. degrees in Computer Science from Sohag University, in 2018. Currently, she is Assistant Professor at the Information Technology Department, Faculty of Computers and Artificial Intelligence, Sohag University, Egypt. Her research interests include, but are not limited to, machine learning, deep learning, natural language processing, computer vision, data mining, cloud computing, cybersecurity, and artificial intelligence applications. She has published many research papers in international journals and conferences and has participated in several collaborative research projects related to IT and AI. She can be contacted at: hanan.hamed@fci.sohag.edu.eg

E. A. Zanaty is the Dean of Faculty of Computers and Artificial Intelligence, Sohag University, Sohag, Egypt. He received his Ph.D. from Chemnitz University of Technology, Germany, in 2003. His research interests include computer graphics, image processing, machine learning, and data mining. He has extensive experience in academic leadership and has served on numerous committees for the Supreme Council of Universities in Egypt. He has published widely in international journals and conferences.

Walaa M. Abd-Elhafiez is an Assistant Professor of Computer Science. She received her Ph.D. degree from Sohag University, Sohag, Egypt. Her research interests include image segmentation, image enhancement, image recognition, image coding, and video coding, and their applications in image processing, machine learning, and artificial intelligence. She has more than 55 published research papers in reputed journals and conferences.